Redox behaviour of Cu-Aβ(4-16) complexes related to Alzheimer's Disease

Authors:

Magdalena Z. Wiloch*, Steven Linfield, Natalia Baran, Wojciech Nogala and Martin Jönsson-Niedziółka*

Institute of Physical Chemistry, Polish Academy of Sciences, Kasprzaka 44/52, 01-224 Warsaw, Poland. Email: mwiloch@ichf.edu.pl (M. Wiloch), martinj@ichf.edu.pl (M. Jönsson-Niedziółka)

Abstract

The development of Alzheimer's Disease (AD) has been linked to abnormal quantities of β-amyloid peptides in the brain. The majority of studies have focussed on Aβ(1-40/42) amyloids and their Cu(II)-Aβ(1-40/42) complexes which are responsible for production of reactive oxygen and nitrogen species (ROS and RNS), which are highly toxic to neurons. According to recent studies on amyloid plaques, Aβ(4-42), which is an N-truncated version of Aβ(1-42), is as prevalent as Aβ(1-42) in the brain. Although Cu(II) ions, bounded by Aβ(4-42), can be oxidized to highly reactive Cu(III) ions, its Cu(II) complexes do not appear to contribute to ROS/RNS formation. In this paper, the pH-dependent voltammetric response of Aβ(4-16)-Cu(II) complexes is investigated to understand the influence of the deprotonation of tyrosine within the complex towards the Cu(II)/Cu(III) reaction. The results will help to better understand the scavenging role of tyrosine in quenching highly reactive Cu(III) ions not only in Aβ(4-x)-Cu(II) complexes but also provide clues to the reactive properties of other tyrosine-containing amyloid-metal complexes.

Introduction

Alzheimer's Disease (AD) is one of the most common causes of dementia and is predicted to affect more than 130 million people by 2050.[1]. The economic cost incurred because of caring for AD were estimated to be USD 600 billion annually. The development of AD has been linked to the presence of abnormal contents of β-amyloid peptides (Aβ) in the brain, which forms neurotoxic dimers, oligomers and plaques as a result of aggregation.[2] To date, the most studied amyloid is Aβ(1-x) (where x refers to 16, 40 or 42 amino acids). However, according to analytical studies,[3] Aβ(4-x) is a major component of plaques, often more prevalent than Aβ(1-x). For this reason, Aβ(4-x) is currently being widely studied.[4–7]

The use of electrochemical methods has become a complementary tool in biochemical studies related to the detection, characterisation and kinetic studies of Aβ peptide aggregation.[8] Cyclic voltammetry (CV), differential pulse voltammetry (DPV) and square wave voltammetry (SWV) are the most commonly used, fast and easy electrochemical techniques to study this processes through the oxidation processes of amino acids present in the peptide chain.[8,9] Of all the amino acids present in the Aβ chain, only three are redox active: histidine (His, H), methionine (Met, M) and tyrosine (Tyr, Y). The changes in voltammetric behaviour related to peak position and current decrease of the peaks corresponding to the oxidation of tyrosine, histidine and methionine allow for investigation of fibrilisation mechanisms not only of full-length Aβ, like Aβ(1-40) and Aβ(1-42) but also shorter fragments (like Aβ(10-20), Aβ(12−28)) or mutants (e.g. Aβ(1-40) Y10F, where the tyrosine moiety is substituted by phenylalanine (Phe, F)).[10–15] Oxidation of tyrosine leads to the formation of stable dityrosine dimers of Aβs, whose importance is widely discussed in the pathogenesis of AD.[16–19] According to Enache and Oliveira-Brett, in the initial step of oxidation, Tyr undergoes a one-electron and one-proton transfer to form the tyrosine phenoxyl radical (Tyr$^{\bullet}$).[20–26] This is a pH-dependent process, occurring at a potential ~ 0.65 V *vs.* Ag/AgCl at pH 7.4. The tyrosyl radical that is formed undergoes hydrolysis and the obtained orthoquinone can later be reduced to a catechol in a two-electron and two-proton process.[20]

Voltammetry is also useful for studying metal-induced conformational changes of Aβ(1-x) as well as Aβ(1-x)-Cu(II) complexes, which are formed in the presence of Cu ions in the brain.[6,27–30] For Aβ(1-16), in the presence of Cu(II) ions, a decrease of the tyrosine oxidation peak current and a shift of the oxidation potential to more positive potentials has been observed.[27] This suggests that the structure of the peptide changes significantly upon complexation of these metal cations. Interaction of redox active copper ions with beta amyloid peptides, both Aβ(1-x) and Aβ(4x) leads to formation of Aβ-Cu(II) complexes which have very different properties. Cu(II) is predominantly coordinated by Aβ(1-x) in a distorted square-pyramidal geometry. Therefore Cu(II) ions attached

to Aβ(1-x) can undergo reduction to Cu(I). This process catalyses the production of reactive oxygen and nitrogen species (ROS and RNS) which are highly toxic to neurons.[31–33] In contrast, Aβ(4-x) form square-planar complexes with Cu(II) ions through its ATCUN (the amino terminal Cu(II)- and Ni(II)-binding motif) sequence, that is, by its N-terminal part consisting of Phe-Arg-His (Scheme 1). Because of this, Aβ(4-16)-Cu(II) undergo Cu(II)/Cu(I) reduction at very negative potential values (below -1 V),[34] unattainable for conditions in the human body, which prevents the formation of ROS and RNS. Additionally, ATCUN-Cu(II) complexes allow Cu(II) to be oxidised to Cu(III),[35] which is strong oxidising species, in a reversible or quasi-reversible one-electron redox process.[36–38] In our previous work we showed that in Aβ(4-16)-Cu(II) complexes in the absence of tyrosine the Cu(II)/Cu(III) reaction is reversible.[6], whereas when Tyr is present in the peptide, the reduction is quenched.

Scheme 1 Structure of the Aβ(4-16)-Cu(II) complex investigated in this work.

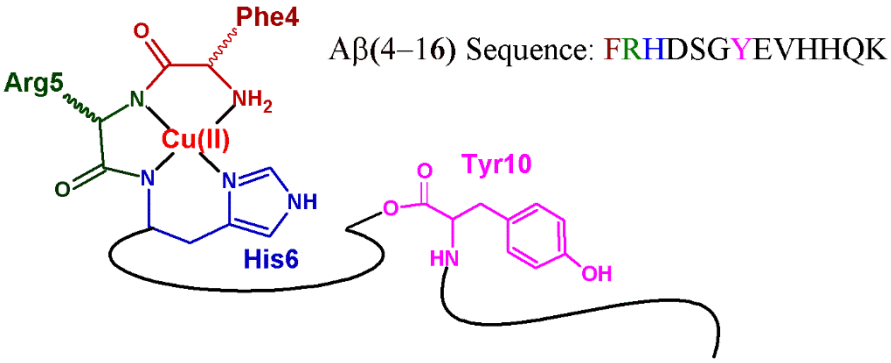

In this paper, the voltammetric response of pH-sensitive Aβ(4–16)-Cu(II) complexes, Aβ(4–16) peptide and tyrosine at different pH values (from 5 to 9) are examined in order to understand the influence of tyrosine (Tyr) deprotonation on the Cu(II)/Cu(III) reaction. Experiments were performed at high (100 Vs^{-1}) and lower scan rates (0.1 Vs^{-1}) (CV) and at different frequencies (SWV) in order to the investigate interaction between Cu(III) and Tyr and determine the rate of this reaction. Additionally, electrochemical studies were supported by simulations. The results will help to better understand the scavenging role of tyrosine in quenching highly reactive Cu(III) ions in Aβ-Cu(II) complexes.

1. Experimental Section

1.1. Chemicals and materials

Inorganic compounds: disodium phosphate (Na_2HPO_4, 99,99%), monosodium phosphate (NaH_2PO_4, 99,99%), sodium hydroxide (NaOH, 99,9%), copper(II) nitrate hydrate ($Cu(NO_3)_2 \cdot xH_2O$, 99,99%), hexaammineruthenium(III) chloride ($[Ru(NH_3)_6]Cl_3$, 98%) and tyrosine (99%) were purchased from Merck and were used without further purification. All solutions used in electrochemical and spectroscopic measurements were prepared with deionised water (resistivity of 18.2 MΩ·cm at 25°C) from a Sartorius purification system. The peptide Aβ(4-16), purchased from Lipopharm, has free N-terminal amines and amidated C-terminus.

1.2. Electrochemical methods

Electrochemical experiments on glassy carbon disk (Ø 3 mm, Mineral) electrodes were performed using Autolab PGSTAT204 potentiostat (Metrohm AG) controlled by the NOVA software (version 2.1.5). CV measurements were performed at different scan rates and at least 3 scans were recorded for each series. The following parameters were used for SWV: step 2 mV, modulation amplitude 50 mV and frequency 25 Hz. The acquisition of voltammetric curves was repeated at least 3 times for each solution of Aβ(4-16)-Cu(II) complex, Aβ(4-16) peptide and tyrosine. All experiments were performed in a three-electrode arrangement, with a Ag/AgCl (3 M NaCl) reference electrode, a platinum rod as the counter electrode, and a glassy carbon disk electrode (GCE) as the working electrode. The reference electrode was separated from the working solution by a salt bridge filled with a 0.1 M phosphate buffer solution, the same pH as in the cell. The potential of the reference electrode was calibrated based on the ruthenium electrode process. The formal potential of hexaammineruthenium(III/II) chloride in 0.5 M KNO_3 is 0.172 ±0.002 V *vs.* Ag/AgCl.[29] Prior to each voltammetric measurement the GCE was polished on a Buehler polishing cloth to a mirror-like surface, using aqueous slurries of 0.05 μm alumina powder followed by 1 min water ultrasonication to remove the remaining powder. All electrochemical measurements were carried out in 0.1 M phosphate buffer solution in the range of pH values from 5 to 9 every half pH unit. For clarity, the curves in main text are shown only for full pH unit increments (pH 5.5, 6.5, 7.4, 8.5). The curves recorded in solutions at pH 5, 6, 7, 8 and 9 are in the SI. In order to support CV data, we have performed SWV experiments at pH 5.5, 6.5, 7.4 and 8.5.

The pH was adjusted by pH-metric titration with small volumes of concentrated NaOH or H_3PO_4 solutions. The concentrations of metal-free Aβ(4-16) and in complexes were 0.5 mM. The ligand-to-copper(II) ratio was 1:0.9 in all cases (a small Cu(II) deficiency helps to avoid interference from

uncomplexed Cu(II) cations). Tyrosine concentration was 0.45 mM. The pH was closely monitored before, during and at the end of each voltammetric measurement.

Cyclic voltammetry experiments on carbon microelectrodes (from ALS CO., Ø 33 μm) were done in a Faraday cage using a PalmSens4 potentiostat controlled by the software PSTrace. These electrochemical measurements were carried out in 0.1 M phosphate buffer solution at pH 6.0 and 7.4.

1.3. UV-Vis spectroscopy

UV-Vis spectra were recorded at 25°C on an Evolution 300 spectrophotometer (Thermo Scientific) over the spectral range of 350– 900 nm. Quartz cuvettes with an optical path of 1 cm were used (Starna scientific). Aβ(4-16) peptide and tyrosine concentrations were determined by UV-Vis absorption of tyrosine (ε276) = 1410 $M^{-1}cm^{-1}$). UV-Vis spectra were also used to control the concentration of Cu(II) solutions. Additionally, UV-Vis spectroscopy was used in order to characterise the Cu(II) complex formation of Aβ(4−16) peptide and metal-free Aβ(4-16) deprotonation in phosphate buffer solutions. Samples containing the peptide with or without Cu(II) ions were titrated with NaOH in the pH range 3–10 by manual additions of the concentrated base solution.

1.4. Computer simulations

Computer simulations of cyclic voltammetry were performed in Comsol 6.0 using the electrochemistry module. The simulations were performed in a 1D geometry with the electrode at one end of the simulation interval and a constant concentration as boundary condition at the other end. The cyclic voltammogram at a scan rate of 5 Vs^{-1} was fitted manually. This high scan rate was chosen because a clear reverse peak could be seen. A more detailed description of the simulations can be found in the SI.

Results and Discussion

Cyclic voltammetry of Aβ(4-16)-Cu(II), Aβ(4-16) and tyrosine

Aβ(4-16) belongs to the ATCUN type peptides and therefore forms stable square planar complexes with Cu(II) ions at pH values above pH 5 (scheme 1A and spectroscopic data SI Figure 1.2). For ATCUN complexes, the Cu(II)/Cu(III) reaction is predicted to occur.[39] Depending on the amino acid sequence, the Cu(II)/Cu(III) process is usually nearly electrochemically reversible (both oxidation and reduction peak are present, and ΔE_p is close to $59/n$ mV at 25 °C) as described for GGH-Cu(II),[38] or quasi-reversible (both oxidation and reduction peak are present, and ΔE_p value is higher than 59 mV at 25 °C) for BAH-Cu(II).[40] However, no reduction signal was observed (Figure 1 A) for the Aβ(4-16)-Cu(II) complex in all pHs when 0.1 Vs^{-1} was applied. The absense of the Cu(III)/Cu(II) peak in the Aβ(4-16)-Cu(II) complex results from the presence of redox active tyrosine in the peptide sequence, which is quenching the Cu(III)/Cu(II) process.[4] As was shown in a previous publication, replacing Tyr by Phe (a non redox active amino acid) resulted in the presence of a Cu(III)/Cu(II) peak for the Aβ-Cu(II) complex.[4] For this reason, we not only investigated the Aβ(4-16)-Cu(II) complex but also oxidation of tyrosine in the peptide (Figure 1 B). Tyrosine oxidation is visible in CVs recorded for the complex, Aβ and for the tyrosine amino acid itself.

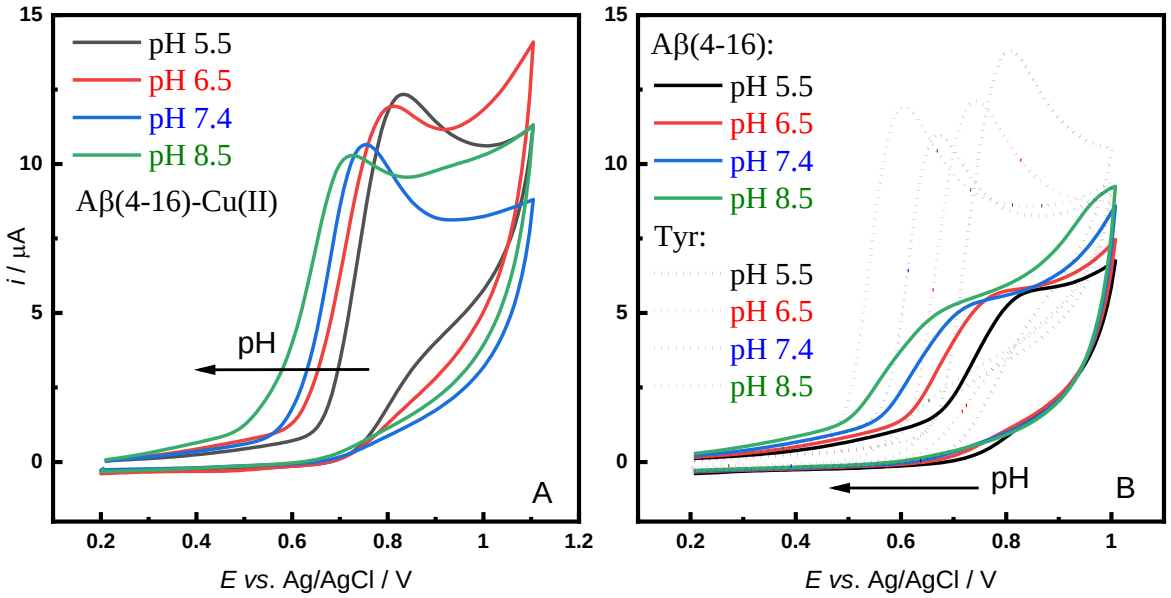

Figure 1 CV (first scan) for (A) **Aβ(4-16)-Cu(II)** complexes (1:0.9 molar ratio) and (B) **Aβ(4-16) and Tyr** at pH range values 5.5 – 8.5 recorded in 0.1 M phosphate buffer, **v = 0.1 V s^{-1}.**

Oxidation of tyrosine in the Aβ sequence is an irreversible process due to the formation of a thermodynamically unstable tyrosyl radical.[20] Therefore on registered CV only anodic peak is present (Figure 1 B). For both the complex and the peptide itself the anodic signal shifted toward less positive potentials as the pH increased, which indicates that a proton exchange occurs in the process. The ratio of number of electrons and protons exchanged was estimated from the $E_{p,ox}$ *vs* pH plots (Figure 2). The oxidation potential for Aβ(4-16) and tyrosine shows a shift of 54 ± 2 and 63 ± 2 mV per pH unit, respectively, indicating a one-electron and one-proton process according to the Nernst equation. In contrast, the slope of 33 ± 1 mV per pH unit obtained for the Aβ(4 16)-Cu(II) complex indicates the transfer of two electrons and one proton (Figure 2). It is likely that the shift in Cu(II)/Cu(III) oxidation potential (which in itself should not be pH dependent) is related to the deprotonation of not only tyrosine but also other amino acids in the peptide sequence, which changes the electrostatic environment around the metal centre and therefore facilitates the oxidation process on the electrode. This phenomena was observed by us earlier for other Cu-peptide complexes.[42] The CVs also show a strong background from the broad oxidation of His which is centred outside the measured electrochemical window (E_{ox} ~1.10 V, *vs.* Ag/AgCl.[9])

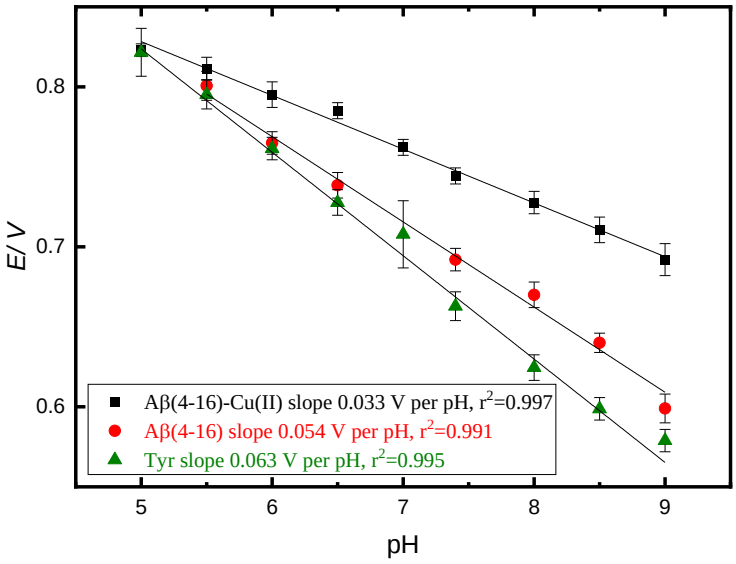

Figure 2 Plot of of $E_{p,ox}$ *vs.* the pH obtained for Aβ(4-16)-Cu(II) (black), Aβ(4-16) (red) and Tyr (green).

Similar studies, aiming to explain the influence of tyrosine on the oxidation process of copper(II) ions, were conducted by Tsai and Weber for tripeptide complex YGG-Cu(II).[41] These authors proposed an electrochemical-chemical (EC) mechanism. Therefore, based on their article, an initial suggestion for a possible mechanism for Aβ(4-16)-Cu(II), where most likely in the first

electrochemical step, tyrosine is deprotonated and oxidised to the radical (Y$^{\bullet}$) and Cu(II) ions are oxidised to the Cu(III), could be:

$$A\beta Y_H\text{-}Cu(II) \xrightarrow{k_1} A\beta Y^{\cdot}\text{-}Cu(III) + H^+ + 2e. \quad (1)$$

This is consistent with our two-electron one-proton data (Figure 2). In the second step (chemical), intramolecular electron transfer may occur between the Cu(III) and the tyrosine radical resulting in:

$$A\beta\text{-}Cu(III)Y^{\cdot} \xrightarrow{k_{homo}} A\beta\text{-}Cu(II)Yox, \quad (2)$$

where AβY$_H$-Cu(II) emphasises the presence of protonated tyrosine in the peptide in a non-oxidised form; AβY$^{\bullet}$-Cu(III) emphasises the presence of tyrosine in the peptide in an oxidized, radical form; and AβYox-Cu(II) emphasizes that the tyrosine was oxidized again by Cu(III) ions (chemical process).

Tsai and Weber never determined the rate of the homogeneous reaction but assumed it would be relatively fast since no reduction peaks were observed in voltammograms, even at 2 Vs^{-1} scan rate.[41] To further investigate the EC mechanism, proposed on the basis of the Tsai and Weber article[41], we carried out additional experiments at increased scan rates. For 5 V/s a standard electrode was used, but carbon fibre microelectrodes (33 μm Ø) were employed to investigate the quenching process at higher scan rates (50 and 100 V s-1). These measurements were performed specifically around the pH range (pH 6 – 7) at which tyrosine deprotonation appeared to have a marked effect on the presence of the cathodic peak.

The carbon fibre microelectrodes had a significantly smaller surface area than the typical macroelectrodes used in the rest of this paper. This allowed cyclic voltammetry to be performed at the higher scan rates without incurring significant capacitive currents (predicted by Eq. 3) which would have complicated the observation of peaks when using the macroelectrodes.

$$i = C \times \upsilon \quad (3)$$

When changing the scan rate, the nature of the mass transport to the microelectrode falls somewhere between the planar diffusion and steady-state diffusion models, represented in Eq. 4 by the left-hand and right-hand terms respectively.

$$j = \frac{nFD^{1/2}c}{\pi^{1/2}t^{1/2}} + \frac{4nFDc}{\pi a} \quad (4)$$

Since the times employed were so short, the left-hand planar diffusion term dominates and no steady state signal from the voltammetry was observed. Instead, an anodic peak corresponding to

Cu(II) oxidation was observed. In such conditions the limiting factor for the observation of a cathodic peak on the return scan is the subsequent quenching of Cu(III) by the tyrosine. By scanning at faster rates, the Cu(III) could be reduced before the quenching could take place, resulting in the observation of a cathodic peak.

As before, the CVs exhibited a single oxidation peak and $E_{p,ox}$ shifting toward less positive potentials as the pH increased (Figure 3 and Table 2 SI). Additionally, on CVs we observed a cathodic peak related to the Cu(III) reduction. Notably, for a scan rate of 5 V/s, the reduction peak was visible in the pH range from 5.0 to 6.5. At pH 7.4 the reduction signal has almost disappeared. Further increase in pH resulted in its complete disappearance. This is most likely due to the fact that at a higher pH, tyrosine deprotonates much faster, and as a consequence, the deprotonated form more easily quenches Cu(III) ions. For scan rates of 50 and 100 V/s the reduction peak is visible also at pH 7.4. So, for short timescales it is possible to reduce the Cu(III) before quenching by tyrosine could take place. (Figure 4).

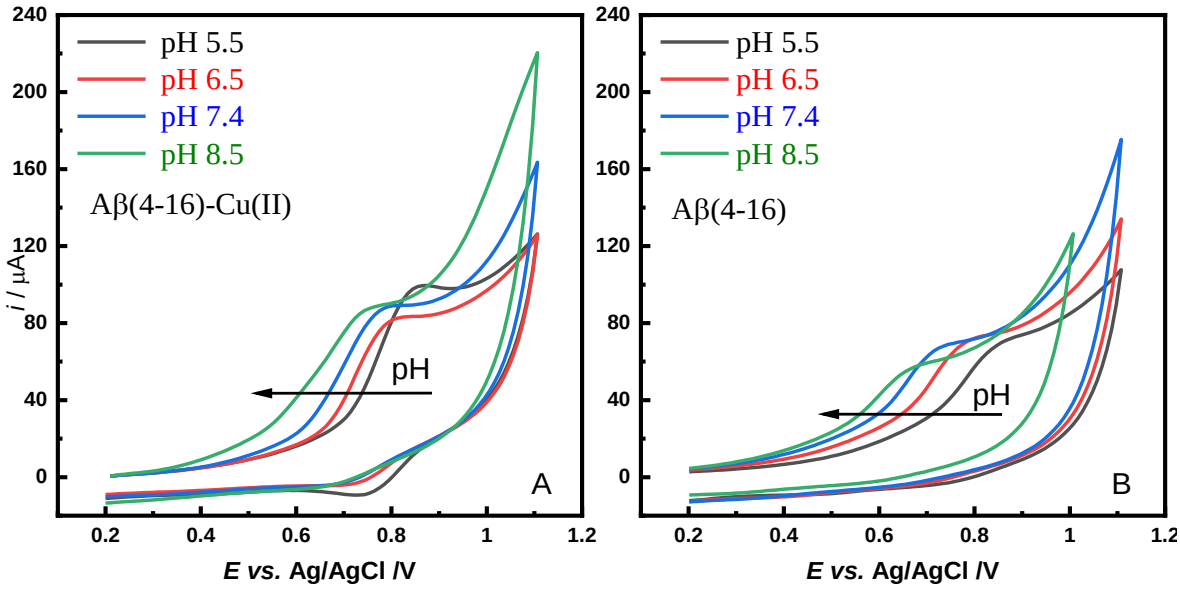

Figure 3 CV (first scan) for (A) **Aβ(4-16)-Cu(II)** complexes (1:0.9 molar ratio) and (B) **Aβ(4-16)** at pH range values 5.5 – 8.5 recorded in 0.1 M phosphate buffer, **v = 5 V s^{-1}.**

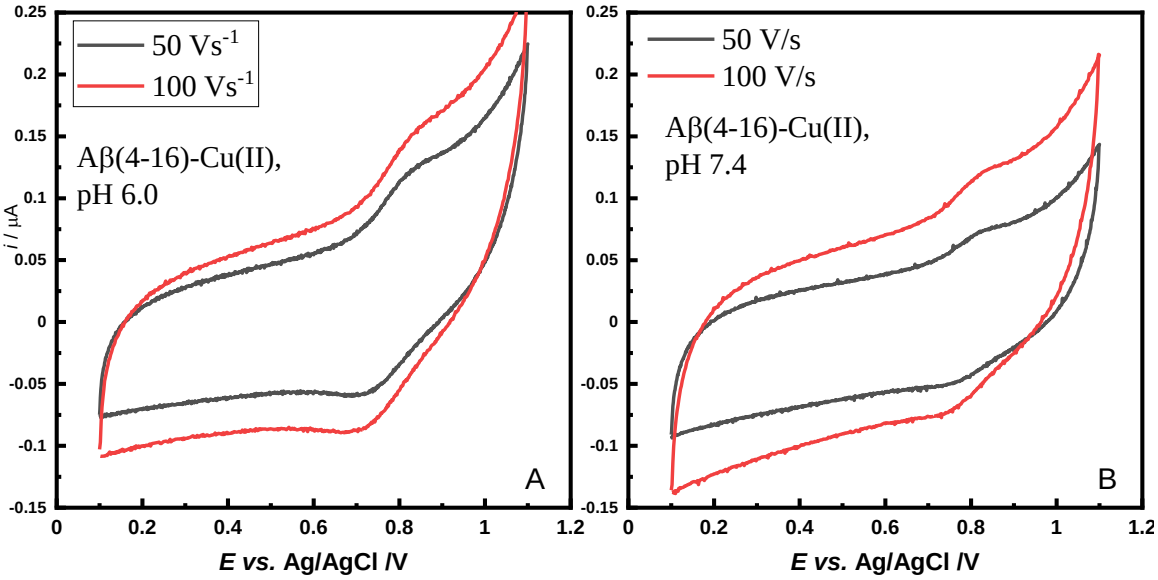

Figure 4 CV obtained for **Aβ(4-16)-Cu(II)** complexes at **pH 6.0** and **pH 7.4 on micro electrodes** recorded in phosphate buffer ν = 50 and 100 Vs^{-1}

These results suggest that the investigated process does not follow a simple EC mechanism. Therefore, we propose a different mechanism for the studied process. In the initial electrochemical step (1) oxidation of tyrosine and Cu(II) ions occur at very similar potentials, especially at lower pH values. However, as the pH increases, tyrosine oxidation occurs at slightly lower potentials compared to Cu(II). Therefore, an obvious widening of the half peak width is seen. Considering this, it might be reasonable to divide the reaction in Eq. 1 into separate steps. While the second step is the same as in EC mechanism. An alternative model is therefore an electrochemical-electrochemical chemical (EEC) mechanism such as the one in eq 5:

(E1 & E2)

$$A\beta Y_H\text{-}Cu(II) \rightleftarrows^{k1} A\beta Y^{\cdot}\text{-}Cu(II) + H^+ + e^- \quad (5a)$$

$$A\beta Y^{\cdot}\text{-}Cu(II) \rightleftarrows^{k2} A\beta Y^{\cdot}\text{-}Cu(III) + e^- \quad (5b)$$

C)

$$A\beta Y^{\cdot}\text{-}Cu(III) \xrightarrow{k_{homo}} A\beta Yox\text{-}Cu(II) \quad (2)$$

After the final step, it looks like the Cu(II) ion in AβYox-Cu(II) could be oxidised back to Cu(III), after which the reduction to Cu(II) should be seen. However, for a scan rate of 0.1 Vs^{-1}, the anodic peak corresponding to the Cu(II)/Cu(III) is visible only in the first cycle (for any pH value). At higher scan rates, which resulted in also the cathodic (Cu(III)/Cu(II)) being present, Cu(II)/Cu(III) oxidation could be seen in each of the 3 measurement cycles (SI Figure 3.8, for 5

V/s). This suggests that the AβYox-Cu(II) undergoes some structural conformation that either changes the Cu(II) binding away from the ACTUN motif that enables the oxidation to Cu(III), or that the Cu is completely released from the peptide. Since Cu(III) is generally not stable in aqueous solutions, we would not expect to see any further oxidation from free Cu. Investigation of these structural changes are underway, but are beyond the scope of this study.

The step

$$\mathrm{A\beta Y_H\text{-}Cu(II)} \rightleftarrows^{k1} \mathrm{A\beta Y_H\text{-}Cu(III)} + e^- \qquad (6)$$

should be possible in principle, but since tyrosine is oxidised at lower potential than Cu(II) for all moderate pH values, it is highly unlikely.

In order to confirm the proposed EEC mechanism, cyclic voltammograms were simulated based the mechanisms described in equations 2–3, as well as SWV experiments. We fitted cyclic voltammograms to the experimental data from pH 5.5 and scan rate 5 Vs^{-1}, where a clear reduction peak is visible. The height of the peak cannot be fitted properly due to the presence of the strong background from oxidation of histidine E_{ox} ~1.10 V, *vs.* Ag/AgCl.[9] The model was fitted manually until a good agreement was found, thus the found values may not be optimal parameter values, but they should be relatively close. The optimised parameters show an ET standard rate constant for both reactions of ca 0.02-0.03 cms^{-1}, but the charge transfer coefficient for the Tyr oxidation (0.23) is significantly lower than for Cu (0.56).

Square wave voltammetry studies

CV results were supported also by SWV experiments in order to investigate both oxidation and reduction processes at fast switching time and determine the rate of the following chemical step of EEC process. Figure 4 (also Figure 3.10 SI), shows the forward and reverse components of SWV, for the Aβ(4-16)-Cu(II) complex~~es~~. In all these cases a small reduction peak is seen in the reverse current. In SWV, a reduction step is applied directly after the oxidation step. This potential program makes it possible to measure a reduction in an EC process, even when the rate of the chemical step is quite fast. For SWV registered for Aβ in the absence of metal, no reduction peak (backward current) is visible, confirming that only Cu(III) ions undergo the reaction in the studied complex. The same is true for SWVs of only the Tyr (Figure 3.10 SI).

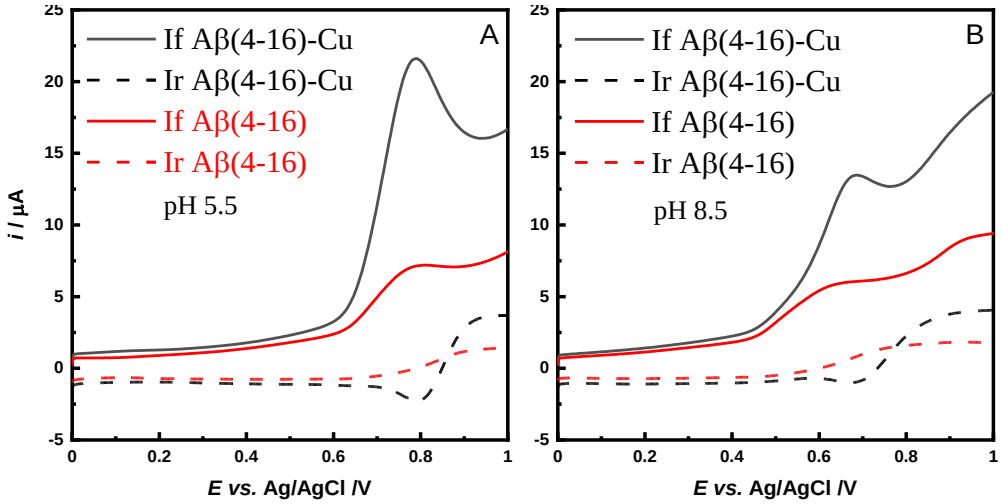

Figure 4 SWV for Aβ(4 16)-Cu(II) complex, Aβ(4-16) at pH 5.5 (A) and 8.5 (B) recorded in 0.1 M phosphate buffers. I_f – forward current (solid lines), I_r – reverse current (dashed lines).

We have additionally performed SWV at different frequencies (from 5 up to 25 Hz) (SI Figure 8.1) in order to determine the rate of the following chemical step, which is an internal electron-transfer from the Cu(III) ion to the Tyr•. As the frequency decreases, the cathodic peak during the reverse current step gradually disappears. The slope in the voltammogram makes it hard to determine the exact frequency when the peak disappears, but it lies between 10 and 15 Hz. This critical frequency is dependent on the rate of the following homogeneous step in an EC reaction mechanism,[43] which in our case corresponds to 30-45 s^{-1}. This is somewhat higher than found in the CV simulations (15 s^{-1}). As the pH increases, the reduction peak disappears. This is likely due to the increase in the amount of deprotonated Tyr, which as discussed above, significantly increases the rate for the intramolecular electron transfer.[41] The SWV results corroborate the CV data that the oxidation of Aβ(416)-Cu(II) complexes is an EEC mechanism, with the rate of the chemical step dependent on the amount of deprotonated tyrosine available.

Conclusions

We investigated the redox properties of copper complexes with Aβ(4–16), which is a good model peptide for Aβ(4–42). On the basis of cyclic and square wave voltammograms as well as computational studies we investigated Cu(II) oxidation to Cu(III) and the influence of the tyrosine moiety on this process. On CVs recorded with lower scan rates (0.1 Vs^{-1}) only the anodic peak for Cu(II)/Cu(III) appeared over the entire range of studied pH (from 5 to 9). The oxidation process Cu(II)/Cu(III) in a complex with Aβ(4-x) appears irreversible due to subsequent chemical reduction. However, a significant increase in the scan rate to 5 Vs^{-1} and higher, revealed the cathodic peak associated with the Cu(III)/Cu(II) process. We performed square wave voltammetry

measurements and simulations based on the recorded CVs to determine the rate of charge transfer reaction between Cu(III) and tyrosine. This process is pH sensitive because with increasing pH the Cu(III)/Cu(II) cathode peak disappears, suggesting that the deprotonation of tyrosine increases the rate of charge transfer between the metal centre and this redox active amino acid. Our findings shed new light on the relevance of the tyrosine moiety in the redox process that may occur when neurodegenerative diseases such as Alzheimer's or Parkinson's disease are developing.

Data access

Data collected for this research is freely available in the repository RepOD[44].

Acknowledgements

This work has been financially supported by the National Science Centre Poland within the Sonatina project 2021/40/C/ST4/00090.

Keywords: Voltammetry • β-amyloid • tyrosine• copper complex• Alzheimer's disease

Bibliography:

[1] E. Stefaniak, W. Bal, *Inorg. Chem.* **2019**, *58*, 13561–13577.
[2] C. Cheignon, M. Tomas, D. Bonnefont-Rousselot, P. Faller, C. Hureau, F. Collin, *Redox Biol.* **2018**, *14*, 450–464.
[3] H. Lewis, D. Beher, N. Cookson, A. Oakley, M. Piggott, C. M. Morris, E. Jaros, R. Perry, P. Ince, R. A. Kenny, C. G. Ballard, M. S. Shearman, R. N. Kalaria, *Neuropathol. Appl. Neurobiol.* **2006**, *32*, 103–118.
[4] M. Mital, N. E. Wezynfeld, T. Frączyk, M. Z. Wiloch, U. E. Wawrzyniak, A. Bonna, C. Tumpach, K. J. Barnham, C. L. Haigh, W. Bal, S. C. Drew, *Angew. Chem. Int. Ed.* **2015**, *54*, 10460–10464.
[5] M. Mital, I. A. Zawisza, M. Z. Wiloch, U. E. Wawrzyniak, V. Kenche, W. Wróblewski, W. Bal, S. C. Drew, *Inorg. Chem.* **2016**, *55*, 7317–7319.
[6] M. Z. Wiloch, U. E. Wawrzyniak, I. Ufnalska, A. Bonna, W. Bal, S. C. Drew, W. Wróblewski, *J. Electrochem. Soc.* **2016**, *163*, G196–G199.
[7] E. Stefaniak, E. Atrian-Blasco, W. Goch, L. Sabater, C. Hureau, W. Bal, *Chem. Weinh. Bergstr. Ger.* **2021**, *27*, 2798–2809.
[8] A.-M. Chiorcea-Paquim, T. A. Enache, A. M. Oliveira-Brett, *Curr. Med. Chem.* **2018**, *25*, 4066–4083.
[9] A.-M. Chiorcea-Paquim, A. M. Oliveira-Brett, *Curr. Opin. Electrochem.* **2022**, *31*, 100837.
[10] T. A. Enache, A. M. Oliveira-Brett, *Bioelectrochemistry* **2017**, *114*, 13–23.
[11] M. Vestergaard, K. Kerman, M. Saito, N. Nagatani, Y. Takamura, E. Tamiya, *J. Am. Chem. Soc.* **2005**, *127*, 11892–11893.
[12] T. A. Enache, A.-M. Chiorcea-Paquim, A. M. Oliveira-Brett, *Anal. Chem.* **2018**, *90*, 2285–2292.
[13] T. A. Enache, A.-M. Chiorcea-Paquim, A. M. Oliveira-Brett, *Anal. Chim. Acta* **2016**, *926*, 36–47.
[14] P. Lopes, M. Xu, M. Zhang, T. Zhou, Y. Yang, C. Wang, E. E. Ferapontova, *Nanoscale* **2014**, *6*, 7853–7857.
[15] E. V. Suprun, S. P. Radko, S. A. Khmeleva, V. A. Mitkevich, A. I. Archakov, A. A. Makarov, V. V. Shumyantseva, *Electrochem. Commun.* **2017**, *75*, 33–37.
[16] X. Huang, R. D. Moir, R. E. Tanzi, A. I. Bush, J. T. Rogers, *Ann. N. Y. Acad. Sci.* **2004**, *1012*, 153–163.

[17] D. G. Smith, R. Cappai, K. J. Barnham, *Biochim. Biophys. Acta BBA - Biomembr.* **2007**, *1768*, 1976–1990.
[18] S. N. Ramteke, Y. P. Ginotra, G. R. Walke, B. N. Joshi, A. S. Kumbhar, S. Rapole, P. P. Kulkarni, *Free Radic. Res.* **2013**, *47*, 1046–1053.
[19] C. S. Atwood, G. Perry, H. Zeng, Y. Kato, W. D. Jones, K.-Q. Ling, X. Huang, R. D. Moir, D. Wang, L. M. Sayre, M. A. Smith, S. G. Chen, A. I. Bush, *Biochemistry* **2004**, *43*, 560–568.
[20] T. A. Enache, A. M. Oliveira-Brett, *J. Electroanal. Chem.* **2011**, *655*, 9–16.
[21] V. Brabec, V. Mornstein, *Biophys. Chem.* **1980**, *12*, 159–165.
[22] J. A. Reynaud, B. Malfoy, A. Bere, *J. Electroanal. Chem. Interfacial Electrochem.* **1980**, *116*, 595–606.
[23] F. E. Ali, K. J. Barnham, C. J. Barrow, F. Separovic, *J. Inorg. Biochem.* **2004**, *98*, 173–184.
[24] J. R. Neyra Recky, M. P. Serrano, M. L. Dántola, C. Lorente, *Free Radic. Biol. Med.* **2021**, *165*, 360–367.
[25] M. Faraggi, M. R. DeFelippis, M. H. Klapper, *J. Am. Chem. Soc.* **1989**, *111*, 5141–5145.
[26] C. Castaño, M. L. Dántola, E. Oliveros, A. H. Thomas, C. Lorente, *Photochem. Photobiol.* **2013**, *89*, 1448–1455.
[27] E. V. Suprun, N. V. Zaryanov, S. P. Radko, A. A. Kulikova, S. A. Kozin, A. A. Makarov, A. I. Archakov, V. V. Shumyantseva, *Electrochimica Acta* **2015**, *179*, 93–99.
[28] M. Z. Wiloch, M. Jönsson-Niedziółka, *J. Electroanal. Chem.* **2022**, *922*, 116746.
[29] M. Z. Wiloch, N. Baran, M. Jönsson-Niedziółka, *ChemElectroChem* **2022**, *9*, e202200623.
[30] N. E. Wezynfeld, A. Tobolska, M. Mital, U. E. Wawrzyniak, M. Z. Wiloch, D. Płonka, K. Bossak-Ahmad, W. Wróblewski, W. Bal, *Inorg. Chem.* **2020**, *59*, 14000–14011.
[31] N. Bodnár, K. Várnagy, L. Nagy, G. Csire, C. Kállay, *J. Inorg. Biochem.* **2021**, *222*, 111510.
[32] C. Amatore, **n.d.**, 14.
[33] R. D. Teo, R. Wang, E. R. Smithwick, A. Migliore, M. J. Therien, D. N. Beratan, *Proc. Natl. Acad. Sci.* **2019**, *116*, 15811–15816.
[34] C. Esmieu, G. Ferrand, V. Borghesani, C. Hureau, *Chem. – Eur. J.* **2021**, *27*, 1777–1786.
[35] Y. Feng, P.-H. Lee, D. Wu, Z. Zhou, H. Li, K. Shih, *J. Hazard. Mater.* **2017**, *331*, 81–87.
[36] K. P. Neupane, A. R. Aldous, J. A. Kritzer, *Inorg. Chem.* **2013**, *52*, 2729–2735.
[37] F. P. Bossu, K. L. Chellappa, D. W. Margerum, *J. Am. Chem. Soc.* **1977**, *99*, 2195–2203.
[38] K. P. Neupane, A. R. Aldous, J. A. Kritzer, *J. Inorg. Biochem.* **2014**, *139*, 65–76.
[39] D. W. Margerum, K. L. Chellappa, F. P. Bossu, G. L. Burce, **n.d.**, 3.
[40] M. Z. Wiloch, I. Ufnalska, A. Bonna, W. Bal, W. Wróblewski, U. E. Wawrzyniak, *J. Electrochem. Soc.* **2017**, *164*, G77.
[41] Hweiyan. Tsai, S. G. Weber, *Anal. Chem.* **1992**, *64*, 2897–2903.
[42] M. Z. Wiloch, U. E. Wawrzyniak, I. Ufnalska, G. Piotrowski, A. Bonna, W. Wróblewski, *PLOS ONE* **2016**, *11*, e0160256.
[43] L. Čižmek, Š. Komorsky-Lovrić, M. Lovrić, *ChemElectroChem* **2015**, *2*, 2027–2031.
[44] Wiloch, Magdalena Z., Linfield, Steven, **2023**, DOI 10.18150/QYPW16.